Available online at www.sciencedirect.com
ScienceDirect
Journal of Power Sources 176 (2008) 102–106
JOURNAL OF POWER SOURCES
www.elsevier.com/locate/jpowsour

Short communication

A high-performance $Gd_{0.8}Sr_{0.2}CoO_3$–$Ce_{0.9}Gd_{0.1}O_{1.95}$ composite cathode for intermediate temperature solid oxide fuel cell

Shouguo Huang *, Chunqiu Peng, Zheng Zong

Ministry of Education Key Laboratory of Opto-electronic Information Acquisition and Manipulation, School of Physics and Materials Science, Anhui University, Hefei, Anhui 230039, PR China

Received 3 September 2007; received in revised form 8 October 2007; accepted 8 October 2007
Available online 13 October 2007

Abstract

Powders of $Gd_{0.8}Sr_{0.2}CoO_3$ (GSC) were prepared by a glycine–nitrate process. Symmetrical cathodes of GSC–$50Ce_{0.9}Gd_{0.1}O_{1.95}$ (GDC) (50:50 by volume) powders were deposited on GDC electrolyte pellets, and the electrochemical properties of the interfaces between the porous cathode and the electrolyte were investigated at intermediate temperature (500–750 °C) using electrochemical impedance spectroscopy. The addition of 50 vol.% GDC to GSC resulted in an additional factor ≈3 decrease in the area-specific resistance (ASR). The ASR values for the GSC–50GDC cathodes were as low as 0.064 Ω cm^2 at 700 °C and 0.16 Ω cm^2 at 600 °C, respectively. The maximum power density of a cell using the GSC–50GDC cathode was 356 mW cm^{-2} at 700 °C.

Keywords: Cathode; Solid oxide fuel cell; Area-specific resistance; Electrochemical impedance spectroscopy

1. Introduction

A solid oxide fuel cell (SOFC) is an energy conversion device which converts chemical energy directly into electric power with high conversion efficiency and negligible pollution. In order to minimize the stringent requirements placed on the balance-of-plant at high temperature, the operating temperature of SOFC should be lowered to intermediate temperature (IT, 500–800 °C) [1,2]. Unfortunately, the cathode resistance increases rapidly when the operating temperature is low [3,4].

(La, Sr)CoO_3 (LSC) is a promising cathode for ITSOFCs due to its high catalytic activity for oxygen reduction and appreciable conductivity [5,6]. However, it has a high thermal expansion coefficient which is mismatched to the common ITSOFC electrolyte material, $Ce_{0.9}Gd_{0.1}O_{1.95}$ (GDC). (La, Sr)(Co, Fe)O_3 (LSCF), with a higher catalytic activity than (La, Sr)MnO_3 (LSM), is considered to be a promising cathode for ITSOFC [7–9]. Its interfacial resistance is approximately 10 times lower than LSM on $(ZrO_2)_{0.92}(Y_2O_3)_{0.08}$ electrolytes, and interfacial resistances for LSCF–GDC cathodes are as low as 0.01 Ω cm^2 at 750 °C and 0.33 Ω cm^2 at 600 °C [10]. Other doped $LaCoO_3$ such as $Sm_{0.5}Sr_{0.5}CoO_3$, $Ba_{0.5}Sr_{0.5}Co_{0.8}Fe_{0.2}O_3$ (BSCF) compositions and their composites also exhibit good cathode performances at 500–700 °C [11–15]. For example, the ASR of the BSCF cathode was as low as 0.055–0.07 Ω cm^2, and peak power density of the cell with the BSCF cathode was approximately 1010 mW cm^{-2} at 600 °C [13]. Unfortunately, these materials do not completely meet all the technological requirements (thermal expansion, ionic conductivity, mechanical stability, cost), which prevent the rapid commercialization of the ITSOFC system.

Bismuth-based composite cathodes exhibit good cathode performances at intermediate temperature, such as Ag-ESB ($Bi_{0.8}Er_{0.2}O_{1.5}$) [16,17], Ag-YSB ($Bi_{0.75}Y_{0.25}O_{1.5}$) [18,19], and $Bi_2Ru_2O_7$ (-ESB) [20,21]. Conductors based on bismuth oxide have much higher oxygen-ion conductivity, and the conductivity of bismuth oxide is approximately two orders of magnitude higher than that of stabilized zirconia. A further and determining advantage of Bi_2O_3 is its favorable catalytic effect on the oxygen dissociation reaction, which is always the first and often limiting step in every electrochemical process involving oxygen transfer. For example, the ASRs of the $Bi_2Ru_2O_7$ and

* Corresponding author. Tel.: +86 551 5108557; fax: +86 551 5846849.
E-mail address: huangsg@ustc.edu (S. Huang).

0378-7753/$ – see front matter © 2007 Elsevier B.V. All rights reserved.
doi:10.1016/j.jpowsour.2007.10.018

$Bi_2Ru_2O_7$-ESB cathodes were as low as 0.4 and 0.03 $\Omega\,cm^2$ at 700 °C, respectively [20,21]. However, longer-term tests of these composite cathodes are needed because of the migration of the silver phase and the stability of bismuth oxide phase at operating temperature.

(Gd, Sr)CoO_3 (GSC) is an excellent mixed electronic conductor and widely used as electrodes and separating membranes for various electrochemical devices [22]. GSC cathodes have good intermediate and low-temperature performances [23–25]. Dyck et al. [26] found that GDC additions to the GSC material resulted in stable composite cathode materials which showed little interaction amongst their constituent phases, and high electrical conductivity was maintained for compositions with excellent thermal expansion matching the GDC electrolyte. Meanwhile the presence of Gd as one of the main constituents in the cathode also reduces the probability of unfavorable reactions with GDC, which itself contains a promising new cathode material for use with GDC. However, details concerning the electrochemical properties of the GSC–GDC composite cathode were not reported in the literature.

The aim of the present study was to obtain more detailed information about the GSC–GDC composite cathode. GDC electrolytes were used in order to determine the feasibility of using these cathodes with this standard electrolyte material. The electrochemical properties of these cathodes were investigated and correlated with the compositions and microstructures.

2. Experimental

$Gd_{0.8}Sr_{0.2}CoO_3$ (GSC) powders were prepared by a glycine–nitrate process (GNP). The stoichiometric amount of Gd, Sr and Co high-purity nitrates were dissolved in distilled water, forming a solution with the concentration of 0.2 M. The solution was heated on a hotplate, with constant stirring, converted to a viscous gel due to evaporation, and ignited to flame, resulting in fine GSC "ash" of a pale-black color. The "ash" was calcined at the temperature from 600 to 900 °C for 4 h to remove any remaining carbon residues and to form a well-crystalline structure. $Ce_{0.9}Gd_{0.1}O_{1.95}$ (GDC) powders were synthesized using an oxalate co-precipitation method (OCM) [27] and GNP, respectively. The powders were fired at 750 °C for 4 h.

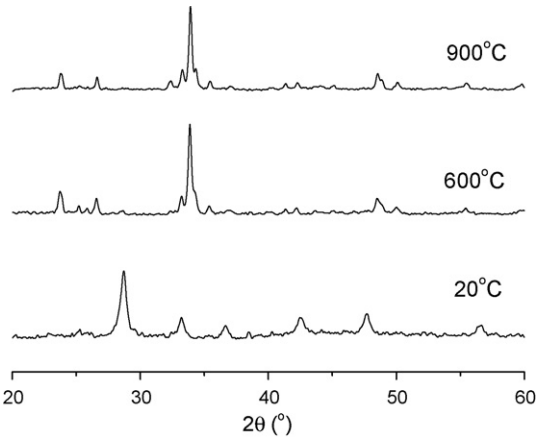

Fig. 1. X-ray diffraction patterns of GSC powders.

In addition to slurry containing 50 vol.% GDC (by GNP), pure GSC slurry was made. These slurries were ball-milled for 24 h, and then screen-printed onto each side of GDC substrates. Both slurries contained the desired amount of GSC and GDC, along with 3 wt.% polyvinyl buteral-76 binder, and 25 wt.% sodium-free corn oil. Methyl ethyl ketone was used as the solvent. The slurries were printed on each side of GDC (by OCM) pellets (15 mm diameter, 0.6 mm thickness, sintering at 1400 °C). The symmetrical cell was sintered at 950 °C for 2 h in air, to form two nominally identical electrodes for electrochemical testing.

Single planar anode-supported thin-film electrolyte fuel cells were fabricated using a dual dry-pressing method for the measurement of cathode property [28]. The anode, formed from a 60:40 wt.% mixture of NiO and GDC (by OCM) powders was dry-pressed into a pellet, and then GDC powders were dis-

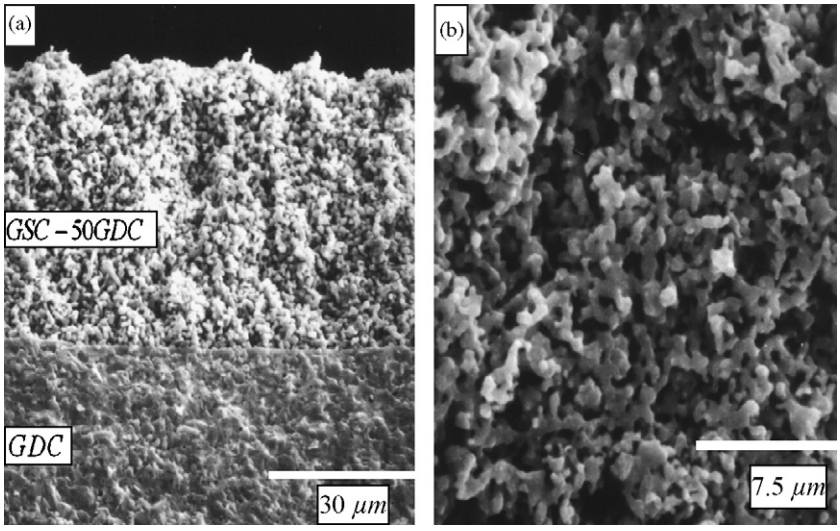

Fig. 2. SEM images of GSC–50GDC cathodes sintered at 950 °C: (a) cross-section and (b) surface.

tributed on the anode surface and co-pressed with the anode. The resultant bilayer was calcined at 1350 °C for 5 h. The fabrication of the LSCF–50GDC (50:50 by volume) cathode was similar to the GSC–50GDC (50:50 by volume). GSC–50GDC and LSCF–50GDC slurries, respectively, were screen-printed on the electrolyte (GDC) surface. The cell with GSC–50GDC was sintered at 950 °C for 2 h, and with LSCF–50GDC was sintered at 950 °C for 2 h. Before measurement of the power density, NiO was reduced to Ni in a H_2 stream at 1000 °C for 1 h. Air and hydrogen humidified with 3 vol.% H_2O were fed to the cathode and the anode sides, respectively.

Impedance spectroscopy measurements were carried out using a CHI604A analyzer. The frequency range was from 0.01 to 10^5 Hz with a signal amplitude of 10 mV. Measurements were taken over a temperature range of 500–750 °C in air.

A scanning electron microscope (SEM, Hitch 650) was used to detect the microstructure of the sintered pellets. The phase identification of GSC powders was made with the powder X-ray diffraction using Cu Kα radiation (D/max-γA, Japan).

3. Results and discussion

Fig. 1 shows the XRD patterns of the as-synthesized ash and calcined GSC powders at varying temperatures. The XRD pattern of the ash sample exhibits all major peaks of a perovskite structure, although the peaks are rather broad. However, all peaks in the XRD pattern of the powder samples calcined at temperatures above 600 °C are relatively sharp. The almost pure perovskite phase can be obtained only after calcinations at 900 °C, which is approximately 300 °C lower than the cal-

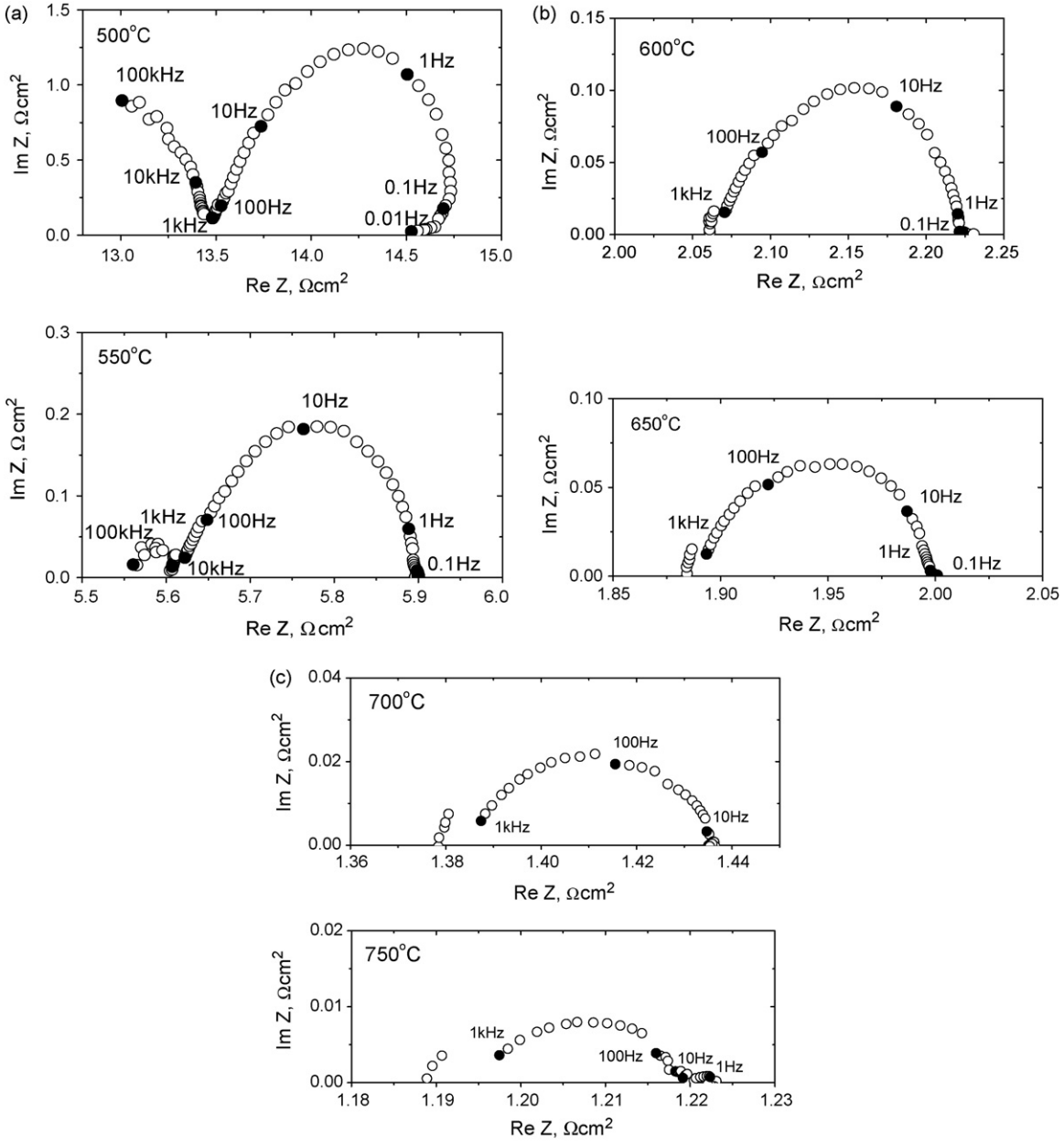

Fig. 3. Impedance spectra of GSC–50GDC cathodes measured from 500 to 750 °C.

cined temperature of the powders synthesized by the traditional solid state reaction. Meanwhile, the XRD pattern of the sintering GSC/GDC sample 1000 °C for 10 h shows the presence of only two crystalline phases, the GDC and the cubic (Gd, Sr)CoO_3 perovskite, and there are no traces of any other phase.

Fig. 2a shows typical cross-SEM images of a GSC–50GDC cathode on a GDC electrolyte, sintered at 950 °C for 2 h. Due to the similar thermal expansion between the two materials, the GSC and GDC particles appear to have sintered well with each other, and show good bonding and continuous contact with the dense electrolyte pellet. The thickness of the cathode layer was found to be 40–50 μm. High porous electrodes were apparent.

Fig. 2b shows the GSC–50GDC interface at higher magnification (4000×) which clearly indicates that the electrode microstructure appeared uniform with reasonable porosity and well-necked particles. The grain size of the GSC–50GDC is of the order of 1.5 μm. The pore sizes appeared to be 1–3 μm.

The evolution of AC impedance spectra for GSC–50GDC cathodes measured at different temperatures in air is shown in Fig. 3. As expected, the increase of the measurement temperature resulted in a significant reduction of the ASR, typically from 0.16 Ω cm^2 at 600 °C to 0.064 Ω cm^2 at 700 °C.

At low temperatures two arcs can be observed at 500 °C. As indicated in Fig. 3, the first arc observed at higher frequency can be associated with the grain (bulk) boundary response of the GDC electrolyte; the second arc at lower frequency comes from the GSC–50GDC cathode. Above 600 °C the grain boundary and bulk processes could not be measured as they became indistinguishable.

For the GSC–50GDC cathode above 600 °C, two arcs were observed between the high- and low-frequency arcs, giving the appearance of a single depressed arc. Attempts were made to fit the impedance arcs for GSC–50GDC. However, overlapping of the arcs made it difficult to deconvolute the impedance spectra with reasonable accuracy. The low-frequency arc is due to concentration polarization caused by the diffusion and exchange of oxygen species to the electrode/electrolyte interface. In general, the low-frequency arc became more dominant with decreasing temperature, which typically indicates that the primary rate-limiting mechanism is diffusion related [29]. This process dominates increases as a function of temperature.

The performance of a mixed conducting cathode is governed by the electronic conductivity of the electrocatalyst, catalytic activities at the triple phase boundary and electrode surfaces, the ionic conductivity of the electrolyte, and rates of transport of gases through the porous electrode. Comparison of ASRs between GSC and GSC–50GDC cathodes was shown in Fig. 4. ASRs of GSC electrodes on GDC electrolytes are relatively high at intermediate temperatures. For example, it is 0.26 Ω cm^2 at 700 °C. This value is much higher than that expected for the cathode ASR, which is lower than 0.15 Ω cm^2 at operating temperature. It was noted that the addition of GDC could dramatically improve the electrochemical performance of GSC, namely decrease the area-specific resistance. The addition of 50 vol.% of GDC to GSC resulted in ASR reduction from 0.26 to 0.064 Ω cm^2 at 700 °C. The addition of 50 vol.% GDC to GSC resulted in an additional factor ≈3 decrease in ASRs. It is possible that the polarization resistance of the optimized composite electrode was decreased by extending the triple phase boundary, which resulted in much lower over potentials toward oxygen reduction, and by increasing the oxygen diffusion upon the addition of an ionic conducting phase (GDC). The results are consistent with those reported by Murray et al. who studied the electrochemical properties of the interfaces between porous composites of LSCF–GDC cathodes and GDC electrolytes from 500 to 750 °C. The addition of 50 vol.% GDC to LSFC resulted in a factor of ≈10 decreases in the polarization resistance [10].

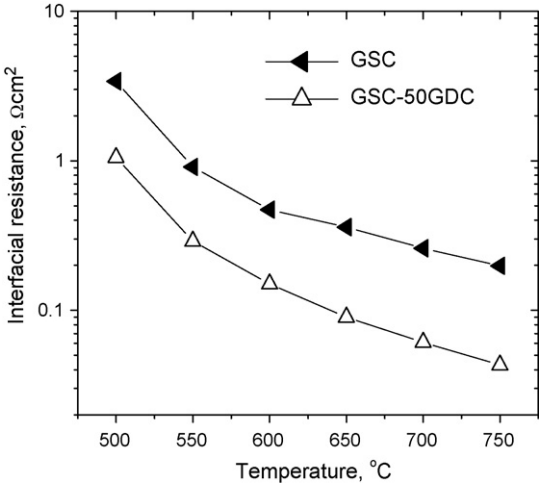

Fig. 4. Comparison of ASRs between GSC and GSC–50GDC cathodes.

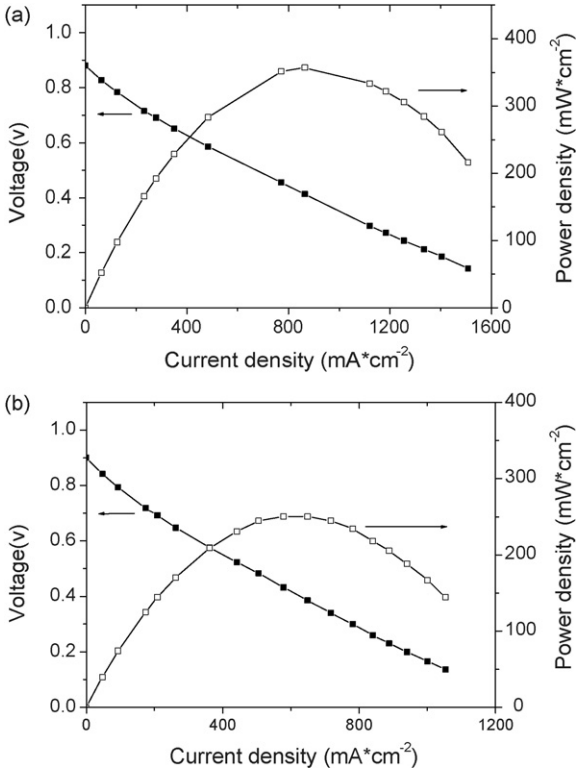

Fig. 5. Cell voltage and power density as functions of current density with (a) GSC–50GDC cathode and (b) LSCF–50GDC cathode.

Fig. 5 shows the power densities as a function of current densities for cells with the GSC–50GDC cathode and the LSCF–50GDC cathode, respectively. The cells were tested at 700 °C with humidified hydrogen as fuel and air as oxidant. The maximum power density of the cell with the GSC–50GDC cathode was 356 mW cm^{-2} at 700 °C, while that with the LSCF–50GDC cathode was only 251 mW cm^{-2}. Power densities are functions of internal resistances, which are the sum of the cathode–anode polarization resistances, and ohmic resistance of the electrolyte. Since the electrolyte and the anode of the two cells are similar, the anodic and electrolyte resistances should be similar. Thus, the relatively higher power densities infer better performance of the GSC–50GSDC electrode.

It is noted that optimization of concentration and better microstructure can further improve the performances of GSC–50GDC cathodes. The results indicated that the GSC–50GDC cathode is a good candidate for operation at or below 700 °C.

4. Conclusions

In this study, the addition of 50 vol.% GDC to GSC resulted in an additional factor ≈3 decrease in the area-specific resistance. The GSC–50GDC cathode exhibits a low over potential and high-activity for oxygen diffusion and dissociation. The ASR of the GSC–50GDC cathode was as low as 0.064 Ω cm^2 at 700 °C, and the GSC–50GDC cathode is promising for ITSOFC operating at or below 700 °C.

Acknowledgement

The authors gratefully acknowledge the fund supported by Anhui Key Laboratory of Information Materials and Devices.

References

[1] N.Q. Minh, J. Am. Ceram. Soc. 76 (1993) 563.
[2] B.C.H. Steele, K.M. Hori, S. Uchino, Solid State Ionics 135 (2000) 445.
[3] B.C.H. Steele, Solid State Ionics 129 (2000) 95.
[4] N.P. Brandon, S. Skinner, B.C. Steel, Annu. Rev. Mater. Res. 33 (2003) 183.
[5] V.V. Srdi, P. Radovan, J. Omorjan, Seydel, Mater. Sci. Eng. B 116 (2005) 119.
[6] T. Horita, K. Yamaji, N. Sakai, H. Yokokawa, A. Weber, E.I. Tiffee, Solid State Ionics 133 (2000) 143.
[7] S. Wang, T. Kato, S. Nagata, T. Honda, T. Kaneko, N. Iwashita, M. Dokiya, Solid State Ionics 146 (2002) 203.
[8] V. Dusastre, J.A. Kilner, Solid State Ionics 126 (1999) 163.
[9] Y. Liu, S. Hashimoto, H. Nishino, K. Takei, M. Mori, J. Power Sources 164 (2007) 56.
[10] E.P. Murray, M.J. Sever, S.A. Barnett, Solid State Ionics 148 (2002) 27.
[11] C.R. Xia, M.L. Liu, Adv. Mater. 14 (2002) 521.
[12] X.G. Zhang, M. Robertsona, S. Yick, C.D. Petit, E. Styles, W. Qu, Y.S. Xie, R. Hui, J. Roller, O. Kesler, R. Maric, D. Ghosh, J. Power Sources 160 (2006) 1211.
[13] Z.P. Shao, S.M. Haile, Nature 431 (2004) 170.
[14] Y.H. Lim, J. Lee, J.S. Yoon, C.E. Kim, H.J. Hwang, J. Power Sources 171 (2007) 79.
[15] S. Lee, Y. Lim, E.A. Lee, H.J. Hwang, J.W. Moon, J. Power Sources 157 (2006) 848.
[16] A. Jaiswal, E. Wachsman, Solid State Ionics 177 (2006) 677.
[17] M. Camaratta, E. Wachsman, Solid State Ionics 178 (2007) 1242.
[18] C.R. Xia, Y.L. Zhang, M.L. Liu, Appl. Phys. Lett. 82 (2003) 901.
[19] H.X. Hu, M.L. Liu, J. Electrochem. Soc. 143 (1996) 859.
[20] A. Jaiswal, E.D. Wachsman, J. Electrochem. Soc. 152 (2005) A787.
[21] V. Esposito, B.H. Luong, E.D. Bartolomeo, E.D. Wachsman, E. Traversa, J. Electrochem. Soc. 153 (2006) A2232.
[22] H.D. Wiemhöfer, H.G. Bremes, U. Nigge, W. Zipprich, Solid State Ionics 150 (2002) 63.
[23] C. Rossignol, J.M. Ralph, J.M. Bae, J.T. Vaughey, Solid State Ionics 175 (2004) 59.
[24] K.T. Lee, A. Manthiram, J. Electrochem. Soc. 153 (2006) 794.
[25] Y. Takeda, H. Ueno, O. Yamamoto, N. Sammes, M.B. Phillipps, Solid State Ionics 86–88 (1996) 1187.
[26] C.R. Dyck, Z.B.H. Yu, V.D. Krstic, Solid State Ionics 171 (2004) 17.
[27] S.W. Zha, C.R. Xia, G.Y. Meng, J. Power Sources 115 (2003) 44.
[28] C.R. Xia, M.L. Liu, J. Am. Ceram. Soc. 84 (2001) 1903.
[29] S.P. Jiang, J.G. Love, Y. Ramprakash, J. Power Sources 110 (2002) 201.